Analyzing Tornado Warning Performance during Individual Storm Life Cycles

JOSUÉ U. CHAMBERLAIN,[a] MATTHEW D. FLOURNOY,[b,c] MAKENZIE J. KROCAK,[d,b,e] HAROLD E. BROOKS,[c,f] AND ALEXANDRA K. ANDERSON-FREY[g]

[a] *Department of Meteorology and Climate Science, San Jose State University, San Jose, California*
[b] *Cooperative Institute for Severe and High-Impact Weather Research and Operations, Norman, Oklahoma*
[c] *NOAA/OAR/National Severe Storms Laboratory, Norman, Oklahoma*
[d] *University of Oklahoma Institute for Public Policy Research and Analysis, Norman, Oklahoma*
[e] *NOAA/NWS/NCEP/Storm Prediction Center, Norman, Oklahoma*
[f] *School of Meteorology, University of Oklahoma, Norman, Oklahoma*
[g] *Department of Atmospheric Sciences, University of Washington, Seattle, Washington*

(Manuscript received 3 August 2022, in final form 8 March 2023, accepted 13 March 2023)

ABSTRACT: The National Weather Service plays a critical role in alerting the public when dangerous weather occurs. Tornado warnings are one of the most publicly visible products the NWS issues given the large societal impacts tornadoes can have. Understanding the performance of these warnings is crucial for providing adequate warning during tornadic events and improving overall warning performance. This study aims to understand warning performance during the lifetimes of individual storms (specifically in terms of probability of detection and lead time). For example, does probability of detection vary based on if the tornado was the first produced by the storm, or the last? We use tornado outbreak data from 2008 to 2014, archived NEXRAD radar data, and the NWS verification database to associate each tornado report with a storm object. This approach allows for an analysis of warning performance based on the chronological order of tornado occurrence within each storm. Results show that the probability of detection and lead time increase with later tornadoes in the storm; the first tornadoes of each storm are less likely to be warned and on average have less lead time. Probability of detection also decreases overnight, especially for first tornadoes and storms that only produce one tornado. These results are important for understanding how tornado warning performance varies during individual storm life cycles and how upstream forecast products (e.g., Storm Prediction Center tornado watches, mesoscale discussions, etc.) may increase warning confidence for the first tornado produced by each storm.

SIGNIFICANCE STATEMENT: In this study, we focus on better understanding real-time tornado warning performance on a storm-by-storm basis. This approach allows us to examine how warning performance can change based on the order of each tornado within its parent storm. Using tornado reports, warning products, and radar data during tornado outbreaks from 2008 to 2014, we find that probability of detection and lead time increase with later tornadoes produced by the same storm. In other words, for storms that produce multiple tornadoes, the *first* tornado is generally the least likely to be warned in advance; when it is warned in advance, it generally contains less lead time than subsequent tornadoes. These findings provide important new analyses of tornado warning performance, particularly for the first tornado of each storm, and will help inform strategies for improving warning performance.

KEYWORDS: Severe storms; Tornadoes; Mesoscale forecasting

1. Introduction

Throughout the United States, tornadoes can form at any given time of the year, most frequently during the spring and early summer (Krocak and Brooks 2018). They present a hazard to the public with deadly outcomes in some cases. It is the responsibility of the National Weather Service (NWS) to issue warnings in advance of developing or existing tornadoes. Unfortunately, isolated[1] tornadoes and the first tornado of the day are the least likely to be warned in advance (Brotzge and Erickson 2010; Krocak et al. 2021b). Factors including atmospheric conditions, geographical location, radar data interpretation, and warning philosophy, among others, may play a role in forecaster confidence and the decision whether or not to issue warnings for storms during severe weather events (Andra et al. 2002; Quoetone et al. 2009; Brotzge et al. 2013; Brotzge and Donner 2013).

In addition to lower probability of detection (POD), more isolated tornadoes also generally have shorter lead time (Brotzge and Erickson 2009). POD is defined as the ratio of

Flournoy's current affiliation: NOAA/NWS/NCEP Storm Prediction Center and the University of Oklahoma, Norman, Oklahoma.

Corresponding author: Matthew Flournoy, matthew.flournoy@noaa.gov

[1] "Isolated" tornadoes in this sense refer to events that are the only one within a single NWS county warning area per day.

DOI: 10.1175/WAF-D-22-0142.1

the number of tornadoes occurring within the time and space of a valid tornado warning to all tornadoes that occurred, and lead time is defined as the time interval between tornado warning issuance and the initial tornado touchdown. These results are consistent with Anderson-Frey et al. (2018), who showed that POD is lower in nontornado outbreak events (59%) and greater in tornado outbreak events (80%). They also attributed higher POD with tornado outbreak events due to atmospheric conditions being more favorable for tornado development. This may lead to increased warning lead time because the storms are likely stronger and more organized with a history of tornadic development (Brotzge and Erickson 2009).

Geographic location also plays an important role in warning performance. Areas that experience more tornado activity generally have a higher POD than areas that experience less tornado activity (Brotzge and Erickson 2010). This is likely due to a combination of human and meteorological factors. Higher POD in areas more frequented by tornadoes may be partly due to heightened forecaster training and education, experience, and situational awareness. Lower POD in areas like Florida and the Gulf Coast may be partially attributable to a higher frequency of generally brief and smaller-scale tornadoes produced by tropical cyclones (Brotzge and Erickson 2010) or nonsupercell tornadoes along sea-breeze fronts. The physical processes associated with the formation of tropical cyclone tornadoes generally remain less understood than those of their inland supercellular counterparts and are an active area of research (e.g., Edwards 2012; Schenkel et al. 2020, 2021). More widespread low-level radar coverage is also generally associated with greater POD and lesser false alarm ratios (FAR; Brotzge and Erickson 2010; Bentley et al. 2021; Kingfield and French 2022; Cho et al. 2022), the fraction of total warnings that are unverified. Average lead times also vary by geographic location for many of the same reasons, with the central United States exhibiting generally greater lead times than other parts of the contiguous United States (Brotzge and Erickson 2009, 2010).

NWS policy and long-term goals can also influence tornado warning performance. For example, tornado warning durations decreased in 2012, yielding reduced FAR (Brooks and Correia 2018). However, this was also associated with a substantial decrease in POD, which would be expected given decreased FAR and resulting in negligible change in overall warning skill (Brooks and Correia 2018, their Fig. 14).

This study aims to investigate how tornado warning performance varies as a function of chronological tornado occurrence (also referred to as "tornado order") in individual storms. This goal extends recent work examining warning performance based on tornado order within each convective day (Krocak et al. 2021b), but not within each individual storm. We present a novel dataset of 3991 tornadoes associated with 75 outbreaks from 2008 to 2014, with each report assigned to an individual storm. Our research questions are as follows:

1) Does POD vary by tornado order within individual storms?
2) Does lead time vary by tornado order within individual storms?
3) Does geographic location or time of day influence POD in addition to tornado order?

In particular, we hypothesize that the POD and lead time associated with the first tornadoes of each storm are lower than subsequent tornadoes produced by the same storm. The remainder of the paper details our exploration of this hypothesis as well as the degree to which other factors like geographic location and time of day may influence the results.

2. Methods

This study analyzes tornado warning performance over the lifetime of individual tornado-producing storms from 2008 to 2014. Due to the time-intensive methods necessitated by this study, we focus on tornado reports that occurred within "tornado outbreaks" as defined by Anderson-Frey et al. (2018). This definition included applying a kernel-density estimation (KDE) clustering to groups of 10 or more tornadoes that occurred no more than 6 h apart (there is no maximum spatial distance in this technique); these groups were then split into outbreaks based on the KDE analysis. The KDE technique smooths the tornado-report map by replacing each tornado report with a Gaussian kernel (see Anderson-Frey et al. 2018; Shafer and Doswell 2011 for more details). This yielded a total of 4103 tornado reports associated with almost all ($n = 75$) outbreaks from 2008 to 2014. Missing radar data prohibited the analysis of three outbreaks during this time period (see appendix A for more details). We analyzed only part of Anderson-Frey et al.'s dataset (which contains data from 2003 to 2015) due to the time constraints of this study. We also did not filter out EF0 tornadoes in order to best preserve the respective orders of each tornado within each storm.

Two different samples of the total tornado report database are used in our analysis. First, 112 reports were removed due to randomly missing variables (e.g., start and end points, start and end times, etc.) which yielded a total of 3991 tornadoes. This is the subset that is plotted in Fig. 1 and used in the ensuing analysis related to POD. Second, 956 of these 3991 tornadoes featured a lead time of "zero" minutes. The actual lead times of these tornadoes could have been either zero or negative minutes, but it is recorded as zero in the database. Because of this, as well as prior work discussing the philosophy of lead-time statistics and the removal of zero-minute lead times (e.g., Brooks and Correia 2018), our analysis of lead time excludes these reports; thus, the subset used to analyze lead-time statistics is comprised of 3035 tornadoes.

Tornado reports and associated verification data (e.g., warned or not warned, lead time, etc.) from 2008 to 2014 were collected from the NWS Verification database.[2] Archived NEXRAD-88D Level-II radar data were downloaded from the online NCEI (National Centers for Environmental

[2] The NWS verification database is available at https://verification.nws.noaa.gov/services/public/index.aspx. NOAA credentials are required for access.

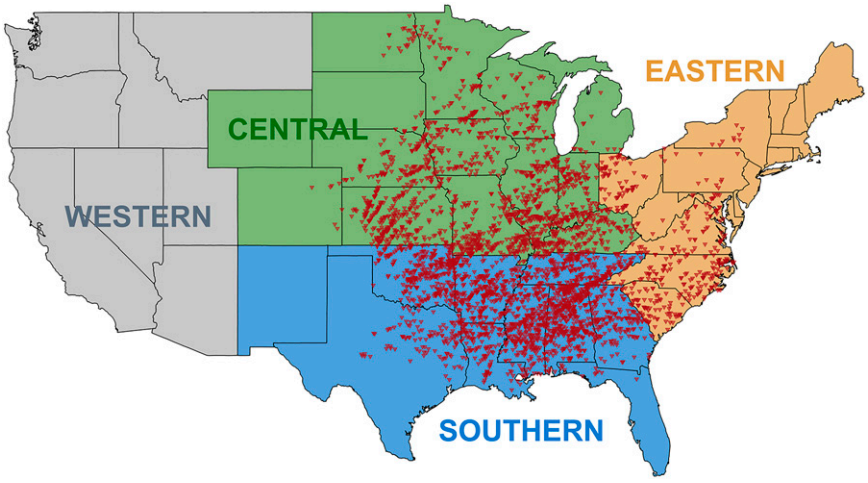

FIG. 1. Map of the 3991 "outbreak" tornado reports from 2008 to 2014 that were paired with storm objects in this study along with NWS regions. Each marker indicates the starting latitude and longitude point of each tornado.

Information) database.[3] GR2-Analyst software[4] was used to manually pair radar-based storm objects with 3991 tornado reports. The reports were associated with a mix of storm modes, including both supercells and QLCSs. This pairing was done by assigning each storm object a number (e.g., 1, 2, 3, etc.) that was then associated with each tornado that each storm produced. Some examples of this process are shown in appendix B. Individual storms were numbered based on the order of initial tornadogenesis for each storm (e.g., the first tornado in time was paired with Storm 1 and the second tornado in time associated with a different storm was paired with Storm 2). All data for each tornado report were paired with the storm objects, including starting and ending locations and times, initial lead time, maximum EF-scale intensity, etc. In a few cases (6 in total), multiple tornadic storms originated from a splitting supercell storm (e.g., Rotunno and Klemp 1985) or primary updraft. The ensuing tornadic storms in these instances were assigned the same storm number as the initial updraft but with a decimal also included (e.g., if storm 10 split into two storms, the new tornadic storms would be classified as 10.1 and 10.2). In some cases, two previously tornadic storms merged into one primary storm that subsequently produced more tornadoes. The ensuing tornadic storm was assigned the minimum of the two storm numbers associated with the two merging storms (e.g., if tornadic storms 7 and 8 merged, the resulting tornadic storm would be identified as storm 7). We chose to combine the storm numbers in this instance because each storm prior to the merger already had a history of producing tornadoes, such that subsequent tornadoes after the merger should not be considered "first" tornadoes (see appendix B for an example).

This study spans a range of convective storm modes including discrete supercells, quasi-linear convective systems (QLCSs), and complex mixed modes. Subjectively tracking individual storm objects was fairly straightforward for discrete modes and primarily relied on reflectivity analysis of the main supercell. Cycling mesocyclones within the same discrete storm were not counted as different storm objects. In the case of QLCSs or mixed modes (e.g., Smith et al. 2012), we also used radial velocity to identify distinct, quasi-steady, tornado-producing updrafts and mesocyclones/mesovortices within the broader convective complex. Each of these quasi-steady circulations were treated as different storm objects. In some cases, cyclic tornadic mesocyclones and mesovortices were treated as the same storm object if they occurred in the same storm-relative location within the broader QLCS. An example of this is provided in appendix B in which two QLCS mesovortices developed and became tornadic within ~5–10 km of each other; in many cases, these events were located within the same tornado warning (at least initially).

Most events were analyzed by the lead author; more complex cases were reviewed on an individual basis by the rest of the team to ensure that our storm-object analyses were consistent across all events. While there is inherent subjectivity involved in the manual assignment of storm objects to tornado reports, our goal was to remain consistent with the research questions, namely, assuming that if the environment and radar depiction remained supportive of tornado production, a human forecaster would be more likely to issue tornado warnings on the resulting storm because the environment had already supported tornado formation earlier.

Once the manual assignment of storm objects to 3991 tornado reports was complete, we grouped tornadoes into chronological groups, including "First," "Middle," "Last," and "Only" tornadoes. Tornadoes in the First and Last groups include the first and last tornado of each storm that produced two or more tornadoes. Middle tornadoes correspond to tornadoes that

[3] The NCEI radar database is available at https://www.ncei.noaa.gov/products/radar.

[4] This software is available for purchase at https://www.grlevelx.com/gr2analyst_2/.

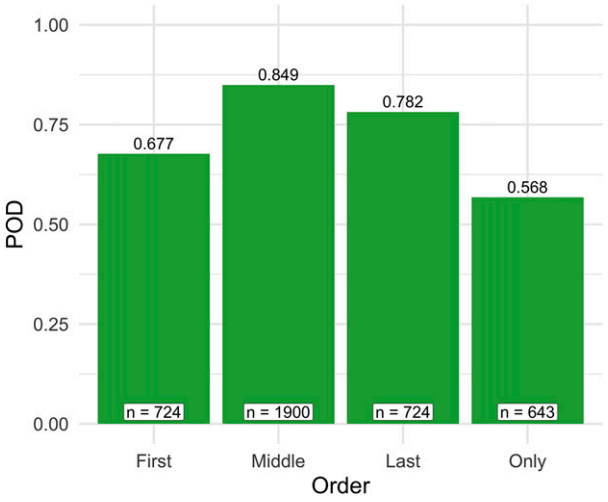

FIG. 2. POD of tornadoes within each tornado chronological group. Sample sizes are shown at the bottom of each bar.

occurred between the first and last tornadoes of each storm (that produced three or more tornadoes). This means that for some storms, the Middle category by definition contained more tornadoes than the First and Last categories. Tornadoes in the Only category were the only ones associated with their storm.

Finally, Fig. 1 shows the start points for all 3991 tornado reports overlaid on the four NWS regions. The starting latitude and longitude points were used to associate each tornado report with one of the four NWS regions (based on the county warning area in which each point resided). Any region-crossing tornadoes were associated with the region that they started in. It was possible for tornadoes from the same storm to be associated with different regions (if the storm crossed a regional boundary). These region designations are distinct from the chronological groups described above.

3. Results

The first tornadoes of each storm are less likely to be warned than subsequent tornadoes (Fig. 2). Across the outbreaks analyzed here, 67.7% of First tornadoes were warned in advance, as opposed to 84.9% of Middle tornadoes and 78.2% of Last tornadoes. Thus, POD increases substantially (almost 0.20) after the first tornado of a storm that produces three or more tornadoes. POD decreases from Middle to Last tornadoes, but not as substantially as the increase in POD from First to Middle tornadoes. The Only tornadoes category exhibited the lowest POD of all groups, which is consistent with the findings of Brotzge and Erickson (2010).

When they are warned in advance, the first tornadoes of each storm contain less lead times than subsequent tornadoes (Fig. 3). The median lead time for First tornadoes is 16 min. This increases to 19 min for Middle tornadoes and 18 min for Last tornadoes. These 2–3-min differences in lead times between First and Middle/Last tornadoes are statistically significant at the 99% confidence interval based on Monte Carlo testing. The median lead time for Only tornadoes (15 min) is similar to that for First tornadoes. Comparisons between these

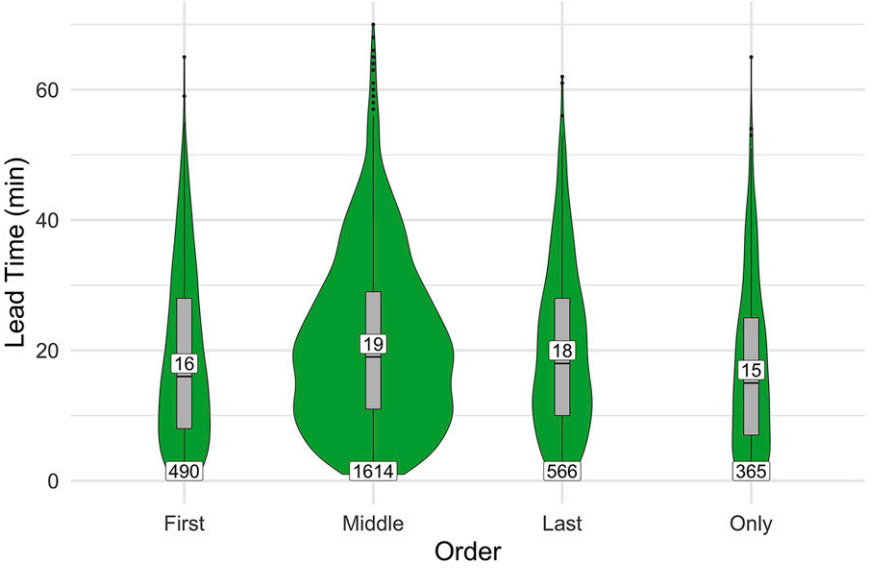

FIG. 3. Violin plots of tornado lead times for all tornadoes within each chronological group that are warned in advance. The body of each violin consists of KDE-smoothed distributions of data. Sample sizes are shown along the bottom of each of the violins. (These sample sizes are different than in Fig. 2 because only tornadoes warned in advance are included here.) Boxplots of each distribution are shown in gray inside each violin. The median lead time is also highlighted with text, and black dots indicate statistical outliers (e.g., Q3 + 1.5 × IQR, where Q3 is the third quartile and IQR is the interquartile range).

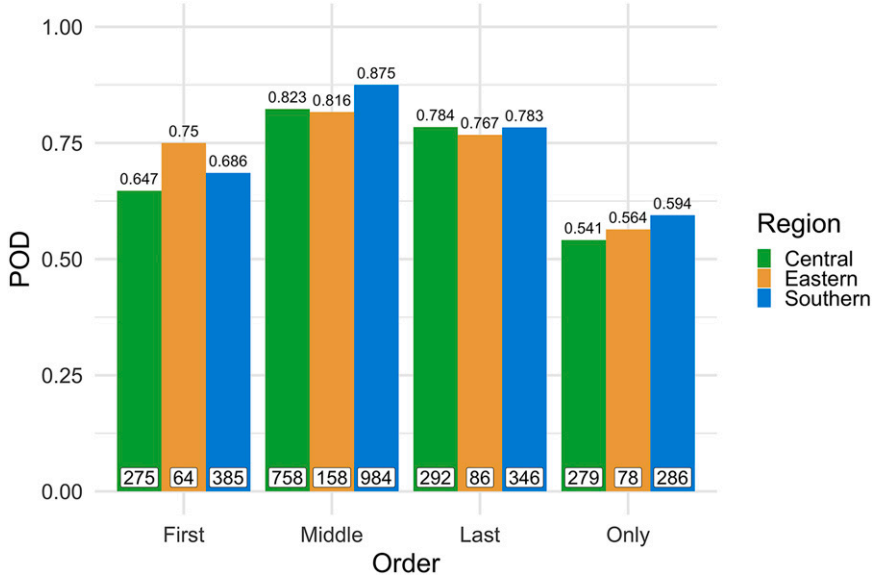

FIG. 4. As in Fig. 2, but with the tornadoes in each group stratified into the NWS Central, Eastern, and Southern geographical regions (see Fig. 1). Sample sizes are shown at the bottom of each bar.

values and the national statistics reported in Brooks and Correia (2018) are presented in section 4.

We then explored if there are any regional differences in tornado warning performance relative to tornado order. Figure 4 shows the same findings in Fig. 2 but stratified by geographical NWS region (Central, Eastern, and Southern). In the case that an ongoing tornado crossed regions (likely a very small number in our dataset), only the starting region is linked with the tornado in this analysis. While tornadoes did occur in the Western Region from 2008 to 2014, none were associated with outbreaks. Many similarities exist when compared to the full dataset, including the fact that in all regions, POD increased from First to Middle tornadoes and then decreased from Middle to Last tornadoes. In all regions, Only tornadoes exhibited lower PODs than any other group. However, small geographical distinctions are also evident; in particular, the POD of First tornadoes ranged from 0.647 in the Central Region to 0.750 in the Eastern Region. We speculate that the larger POD for First tornadoes in the Eastern Region may be due to the limited sample size there and/or differences in forecasting experience and philosophy in areas that are less prone to tornado occurrence. The increase in POD from First to Middle tornadoes also varied by region: 0.176 in the Central Region, 0.066 in the Eastern region, and 0.189 in the Southern Region. Thus, roughly two-thirds of First tornadoes are warned in advance (particularly in the Central and Southern Regions), but this fraction increases substantially with subsequent tornadoes.

Last, we examined if the local diurnal cycle influences tornado warning performance relative to tornado order. Figure 5 shows that for all tornadoes, particularly First and Middle, POD is lower overnight (from local sunset to local sunrise) than during the day (from local sunrise to local sunset). The POD of First tornadoes is 0.087 higher during the day (0.706) than overnight (0.619). The increase in POD from First to Middle tornadoes is similar during the day and night (0.187 and 0.172, respectively). POD for Last and Only tornadoes is slightly more similar when comparing daytime and nighttime tornadoes (0.058 and 0.065, respectively), but POD is still greater during the day. Finally, the drop in POD from Middle to Last tornadoes is twice as much during the day (0.086) than overnight (0.042).

4. Discussion

This is the first study that we are aware of to examine tornado warning performance during the life cycles of individual tornado-producing storms. It is useful to compare the statistics presented here with past similar work on larger spatiotemporal scales. The PODs of First and Only tornadoes—0.677 and 0.558, respectively—are similar to the range of annual 2008–14 PODs for all tornadoes (0.469–0.673; Brooks and Correia 2018). The PODs of Middle and Last tornadoes—0.849 and 0.782, respectively—are larger. Brooks and Correia (2018) found that the mean lead time for tornadoes warned in advance is approximately constant over long periods of time (18.5 min from 1986 to 2011 and around 15 min since then). The 15–16-min lead time for First and Only tornadoes is near the lower end of this range, and the lead times for Middle and Only tornadoes—19 and 18 min, respectively—are near the upper end.

Cumulatively, the statistics presented here demonstrate more tornado warning skill (i.e., contain greater POD and lead times) than the metrics for all tornadoes likely because we focused only on tornadoes that occurred during outbreaks. Outbreaks are typically supported by more volatile environments, a greater

FIG. 5. As in Fig. 4, but with the tornadoes in each group stratified by the time of day that they occurred. "Daytime" tornadoes started between local sunrise and local sunset, and "nighttime" tornadoes started between local sunset and local sunrise. Sample sizes are shown at the bottom of each bar.

expectation of tornado occurrence, and higher-end tornado-watch probabilities, which are all associated with increased warning performance (Anderson-Frey et al. 2016; Krocak and Brooks 2021). In fact, the difference in POD between First (0.677) and Middle/Last tornadoes (0.849/0.782, respectively) is similar to the difference in POD between tornadoes that occurred inside any type of severe thunderstorm or tornado watch (~0.6) and those that occurred within Particularly Dangerous Situation tornado watches (~0.8) from 2008 to 2014 (Krocak and Brooks 2021, their Fig. 1).

The POD of First (0.619) and especially Only (0.530) tornadoes overnight are among the lowest of any chronological group during the day or night. Interactions between a tornadic storm and its local environment during and just after the early-evening transition can be complex (e.g., Coffer and Parker 2015) and can yield brief periods of increased tornadic activity near the onset of nighttime (Anderson-Frey et al. 2016; Krocak and Brooks 2018). On one hand, these results might support continuing to issue tornado warnings on storms during the afternoon, prior to sunset, until the storm sufficiently weakens. However, this mindset is not generally supported by our finding that during the day, the POD of Last tornadoes (0.807) is less than Middle tornadoes (0.893). This result is slightly different for nocturnal tornadoes, in which the PODs of Middle (0.791) and Last tornadoes (0.749) are more similar. This may suggest that forecasters are more likely to try to anticipate tornado demise (or the last tornado of a storm) during the day than overnight.

Diurnal tornado warning skill (in terms of POD and FAR) peaks during the early evening transition, but tornadoes later at night after the early evening transition are typically characterized by very high FAR (Anderson-Frey et al. 2016). This is likely due to a number of meteorological as well as human factors as the convective environment typically becomes more complex and visual storm-spotting becomes limited, for example. Nocturnal tornadoes are also associated with decreased human response and increased human vulnerability and fatalities (Ashley et al. 2008; Krocak et al. 2021a). In the context of these previous studies, our findings suggest that further investigation of tornado warning performance on a storm-by-storm basis will continue to shed light on important physical and warning processes related to the daytime to nighttime transition.

More generally, why do POD and lead time drop slightly from Middle to Last tornadoes, especially during the day? The reason is not immediately clear based on our work. While it may seem logical to continue issuing a tornado warning for a storm until confirmation that the tornado threat has ended, this work indicates that this is not necessarily happening given the lower POD and lead time for Last tornadoes. The slight drop in POD also does not appear to be related to the number of storms that each storm produces. Future work should examine if other meteorological and social differences, such as rotating shifts and different forecasting philosophies, may explain why this pattern is observed for warning performance for Middle and Last tornadoes.

These results are consistent with findings of Brotzge and Erickson (2009, 2010) and Krocak et al. (2021b): the first tornado of each convective day (1200–1159 UTC) during tornado outbreaks is more poorly warned than the rest. Furthermore, we show that this trend more generally extends to the first tornadoes *of each storm*. This implies that tornado warning skill does not necessarily increase after the event has started, at least for individual storms. Instead of assuming future storms will follow a similar tornado-producing evolutionary path, it appears that warning decisions are made on a storm-by-storm basis (Smith et al. 2015). This is consistent with operational forecaster experience (e.g., Smith et al. 2015; Bentley et al. 2021; Bunkers et al. 2022) as well as recent observational (e.g., Klees et al. 2016) and modeling (Coffer et al. 2017; Flournoy et al. 2020; Markowski 2020) work showing that a range of storm- and tornado-scale outcomes are possible within a broader, generally homogeneous environment. This paper indirectly addresses this topic from the human/forecaster perspective and continues to suggest that increased quantification of the range of storm-scale outcomes in similar (and different) meteorological scenarios would be beneficial to the community.

5. Summary and conclusions

The goal of this study was to analyze tornado warning performance on a storm-by-storm basis during tornado outbreaks. This extends prior work examining tornado warning performance on the annual (e.g., Brooks and Correia 2018), and daily (e.g., Brotzge and Erickson 2009; Krocak et al. 2021b) time scales. To do this, we manually paired tornado reports from the NWS Verification Database with subjectively defined storm objects identified using Level-II NEXRAD 88D radar data. We did this for 3991 tornado reports that were associated with 75 tornado "outbreaks" (as defined in Anderson-Frey et al. 2018) from 2008 to 2014. This approach allowed us to address questions such as the following: is POD lower for the first tornado of each storm ("First") compared to subsequent (e.g., "Middle" and "Last") tornadoes? Is the same true for lead time? Does geographic location or time of day influence whether First tornadoes are more or less poorly warned than subsequent tornadoes?

Our main findings are summarized below:

- *The first tornadoes of each storm are less likely to be warned than subsequent tornadoes in the same storm.* First tornadoes are warned in advance 67.7% of the time as opposed to 84.9% and 78.2% for Middle and Last tornadoes, respectively.
- When they are warned in advance, the first tornadoes of each storm are associated with less lead time than subsequent tornadoes produced by the same storm. Warnings for First tornadoes have a median lead time of 16 min as opposed to 19 and 18 min for Middle and Last tornadoes, respectively.
- *Storms that only produce one tornado are the most poorly warned.* "Only" tornadoes are warned in advance just over half of the time (POD = 0.568) with a median lead time of 15 min.
- *POD decreases overnight for tornadoes in all chronological groups.* The PODs for First, Middle, and Last tornadoes decrease by roughly 0.06–0.10 for all groups.
- Tornado timing within the day or night does not strongly influence relationships between warning characteristics of different chronological groups. POD decreases overnight for all tornadoes, but the POD for First tornadoes (0.619) is still substantially lower than Middle (0.791) and Last tornadoes (0.749). Just over one-half of nocturnal Only tornadoes (53.0%) are warned in advance.
- Geographic location does not strongly influence the general relationships between warning characteristics of different chronological groups. PODs of First and Only tornadoes are lower than Middle and Last tornadoes in the NWS Central, Southern, and Eastern Regions.

These findings are drawn from the first examination of tornado warning performance during individual storm life cycles within tornado outbreaks. They highlight some of the strengths, weaknesses, and limits of practical predictability in the current tornado-warning paradigm. Even in volatile environments supportive of tornado outbreaks, the first tornadoes *of each storm* (not just the first of each outbreak) are more poorly warned than subsequent tornadoes from the same storm. This has important implications as the severe weather community continues to experiment with new probabilistic formats and warn-on-forecast systems (e.g., Skinner et al. 2018; Calhoun et al. 2021; Wilson et al. 2021; Trujillo-Falcón et al. 2022; Gallo et al. 2022).

We also believe these findings motivate continued study of the evolution of tornadic storms, particularly in their early stages of development. Our study shows that initial tornado occurrence improves downstream predictability. Thus, increased investigation of the initiation and early evolution of potentially tornadic storms might also improve downstream understanding and predictability. Planned future work in this area will analyze tornado warning performance before and after each storm produces tornadoes (i.e., to investigate FAR), including a focus on how this performance may vary based on tornado damage ratings (e.g., comparing weak EF0–1, strong EF2–3, and violent EF4–5 tornadoes). We also look forward to results from ongoing modeling efforts (e.g., LeBel and Markowski 2023; Flournoy and Rasmussen 2022, manuscript submitted to *Mon. Wea. Rev.*; Peters et al. 2022a,b) and field observing campaigns that will further our understanding of processes influencing convection initiation and early evolution.

Acknowledgments. The first author was supported by the University of Oklahoma Research Experience for Undergraduates (REU) program and the NOAA Cooperative Science Center in Atmospheric Sciences and Meteorology research program through the NOAA Educational Partnership Program (NA16SEC4810006). This work was also funded by NOAA under the NOAA–University of Oklahoma Cooperative Agreement NA21OAR4320204, U.S. Department of Commerce. We are grateful for the efforts of Dr. Daphne LaDue, Alex Marmo, and others who help organize and run these programs, as well as

TABLE A1. List of the 112 "outbreak" tornado reports that were omitted from this study due to spatiotemporal errors.

Outbreak ID	WFO	Start time	State	EF rating	Start latitude (°)	Start longitude (°)	End latitude (°)	End longitude (°)
1	LSX	0150 UTC 8 Jan 2008	MO	0	38.39	−91.64	38.39	−91.64
2	OHX	0210 UTC 6 Feb 2008	TN	1	35.38	−88.02	35.46	−87.9
2	OHX	0220 UTC 6 Feb 2008	TN	1	35.46	−87.9	35.48	−87.89
2	PAH	0224 UTC 6 Feb 2008	MO	1	36.7	−90.14	36.73	−89.97
2	LMK	0527 UTC 6 Feb 2008	KY	2	37.7	−85.78	37.7	−85.76
2	LMK	0538 UTC 6 Feb 2008	KY	0	37.99	−85.42	38	−85.41
2	LMK	0552 UTC 6 Feb 2008	KY	0	38.12	−85.05	38.12	−85.05
2	OHX	0632 UTC 6 Feb 2008	TN	0	36.01	−87.32	36.01	−87.32
2	OHX	0712 UTC 6 Feb 2008	TN	0	36.35	−86.67	36.37	−86.62
2	OHX	0722 UTC 6 Feb 2008	TN	1	36.4	−86.54	36.5	−86.37
3	BMX	2217 UTC 17 Feb 2008	AL	1	31.71	−85.67	31.87	−85.36
3	BMX	2238 UTC 17 Feb 2008	AL	0	31.74	−85.29	31.75	−85.29
4	CAE	2252 UTC 15 Mar 2008	SC	2	34.13	−80.32	34.08	−80.08
5	DVN	2330 UTC 10 Apr 2008	IL	1	40.28	−91.31	40.3	−91.28
5	DVN	2333 UTC 10 Apr 2008	IL	0	40.33	−91.28	40.33	−91.28
5	DVN	2335 UTC 10 Apr 2008	IL	0	40.4	−91.24	40.4	−91.23
6	FSD	0042 UTC 2 May 2008	IA	0	43.14	−95.87	43.14	−95.87
6	MEG	2125 UTC 2 May 2008	TN	2	35.96	−89.67	35.97	−89.65
6	OHX	0457 UTC 3 May 2008	TN	1	36.38	−87.54	36.38	−87.53
6	OHX	0500 UTC 3 May 2008	TN	1	36.39	−87.53	36.39	−87.53
6	OHX	0505 UTC 3 May 2008	TN	1	36.42	−87.51	36.43	−87.51
6	OHX	0510 UTC 3 May 2008	TN	1	36.5	−87.38	36.51	−87.37
8	TSA	2219 UTC 10 May 2008	OK	0	35.46	−95.48	35.46	−95.48
8	FFC	1011 UTC 11 May 2008	GA	0	32.75	−83.63	32.75	−83.62
10	DDC	2147 UTC 25 May 2008	KS	0	38.55	−99.06	38.56	−99.05
10	DDC	2149 UTC 25 May 2008	KS	0	38.5	−99.22	38.5	−99.2
11	GID	2302 UTC 29 May 2008	KS	1	39.21	−99.61	39.21	−99.56
11	DMX	0223 UTC 30 May 2008	IA	1	42.4	−94.45	42.4	−94.4
11	DMX	0225 UTC 30 May 2008	IA	0	42.28	−94.43	42.28	−94.39
12	LBF	0010 UTC 6 Jun 2008	NE	0	40.43	−101.16	40.43	−101.16
17	FFC	2245 UTC 18 Feb 2009	GA	0	32.49	−84.15	32.49	−84.08
17	TAE	0550 UTC 19 Feb 2009	GA	2	30.8	−84.18	30.81	−84.08
17	TAE	0555 UTC 19 Feb 2009	GA	2	30.81	−84.08	30.81	−83.91
17	TAE	0620 UTC 19 Feb 2009	GA	3	30.82	−83.8	30.82	−83.77
18	IWX	2115 UTC 8 Mar 2009	IN	1	41.17	−85.48	41.17	−85.48
20	OHX	1719 UTC 10 Apr 2009	TN	4	35.76	−86.85	35.91	−86.28
20	CAE	0153 UTC 11 Apr 2009	GA	0	33.46	−82.44	33.46	−82.43
23	LSX	1705 UTC 8 May 2009	MO	0	37.62	−90.28	37.62	−90.28
23	LSX	1710 UTC 8 May 2009	MO	1	37.52	−90.24	37.52	−90.23
23	PAH	1818 UTC 8 May 2009	IL	0	37.89	−89.12	37.89	−89.12
23	PAH	1845 UTC 8 May 2009	IL	1	37.9	−88.78	37.86	−88.76
23	PAH	1848 UTC 8 May 2009	IL	1	37.86	−88.76	37.83	−88.73
23	MRX	2240 UTC 8 May 2009	TN	0	36.36	−83.8	36.37	−83.79
23	MRX	2336 UTC 8 May 2009	TN	0	36.36	−83.42	36.41	−83.34
23	RLX	0100 UTC 9 May 2009	VA	0	37.19	−82.48	37.19	−82.47
26	OHX	2315 UTC 24 Apr 2010	TN	1	35.65	−87.52	35.67	−87.5
29	GLD	1827 UTC 10 May 2010	KS	1	38.49	−101.21	38.49	−101.19
29	GLD	1831 UTC 10 May 2010	KS	0	38.56	−101.2	38.57	−101.18
29	GLD	1850 UTC 10 May 2010	KS	0	38.82	−101.24	38.83	−101.22
29	DDC	1900 UTC 10 May 2010	KS	0	38.5	−100.7	38.5	−100.7
29	DDC	2008 UTC 10 May 2010	KS	0	38.58	−100.08	38.58	−100.07
29	OUN	2146 UTC 10 May 2010	OK	0	35.72	−97.75	35.72	−97.75
29	OUN	2146 UTC 10 May 2010	OK	0	35.73	−97.74	35.8	−97.67
29	OUN	2154 UTC 10 May 2010	OK	0	35.8	−97.67	35.8	−97.67
29	ICT	2208 UTC 10 May 2010	KS	1	37.1	−96.97	37.1	−96.96
29	OUN	2244 UTC 10 May 2010	OK	0	34.11	−97.75	34.12	−97.72
32	FGF	2038 UTC 17 Jun 2010	ND	0	47.58	−97.8	47.64	−97.78
32	FGF	2235 UTC 17 Jun 2010	ND	1	48.09	−97.69	48.15	−97.72
33	IWX	1421 UTC 26 Oct 2010	IN	0	41	−85.6	41	−85.6

TABLE A1. (*Continued*)

Outbreak ID	WFO	Start time	State	EF rating	Start latitude (°)	Start longitude (°)	End latitude (°)	End longitude (°)
33	IWX	1422 UTC 26 Oct 2010	IN	0	41	−85.6	41.02	−85.58
33	LMK	1635 UTC 26 Oct 2010	KY	0	38.7	−85.4	38.72	−85.39
35	PAH	2025 UTC 31 Dec 2010	MO	2	36.82	−90.52	36.82	−90.52
36	HUN	1818 UTC 28 Feb 2011	TN	2	35.31	−86.11	35.28	−86.28
36	MRX	1930 UTC 28 Feb 2011	TN	1	35.18	−85.28	35.18	−85.28
36	CAE	0024 UTC 1 Mar 2011	SC	1	34.25	−81.73	34.24	−81.67
38	RNK	0525 UTC 5 Apr 2011	NC	1	36.4	−80.57	36.41	−80.53
40	ICT	2311 UTC 14 Apr 2011	KS	0	37.44	−96.55	37.44	−96.55
40	OUN	0136 UTC 15 Apr 2011	OK	1	34.34	−96.08	34.36	−96.07
42	IND	0254 UTC 20 Apr 2011	IN	1	38.53	−87.53	38.48	−87.72
44	SHV	1405 UTC 25 Apr 2011	AR	0	33.63	−93.8	33.7	−93.69
45	OHX	1050 UTC 27 Apr 2011	TN	1	35.41	−87.32	35.43	−87.28
45	MRX	1245 UTC 27 Apr 2011	TN	2	35.3	−84.96	35.32	−84.92
45	MRX	1926 UTC 27 Apr 2011	TN	1	35.4	−85.37	35.43	−85.32
45	MRX	1930 UTC 27 Apr 2011	TN	1	35.43	−85.32	35.44	−85.3
45	MRX	2335 UTC 27 Apr 2011	TN	0	35.18	−84.87	35.19	−84.86
45	MRX	0228 UTC 28 Apr 2011	TN	2	35.36	−85.39	35.4	−85.33
46	BIS	0141 UTC 23 May 2011	ND	0	48.73	−101.71	48.73	−101.71
48	EAX	1635 UTC 23 May 2011	MO	0	38.62	−94.3	38.62	−94.3
48	EAX	1638 UTC 23 May 2011	KS	0	38.96	−94.73	38.96	−94.73
48	IWX	1926 UTC 23 May 2011	OH	0	40.88	−84.6	40.88	−84.6
48	PAH	2151 UTC 23 May 2011	MO	0	37.64	−90.1	37.64	−90.09
48	PAH	2158 UTC 23 May 2011	MO	0	36.53	−90.71	36.54	−90.7
48	CLE	2330 UTC 23 May 2011	OH	0	41.1	−81.55	41.13	−81.48
49	GLD	2325 UTC 20 Jun 2011	KS	0	39.88	−100.25	39.88	−100.25
49	GLD	2344 UTC 20 Jun 2011	KS	0	39.84	−100.15	39.84	−100.15
49	GLD	2345 UTC 20 Jun 2011	KS	0	39.84	−100.18	39.84	−100.18
52	PAH	1157 UTC 29 Feb 2012	KY	1	37.91	−87.55	37.91	−87.52
52	LMK	1605 UTC 29 Feb 2012	KY	2	37.56	−85.77	37.56	−85.72
53	HUN	2045 UTC 2 Mar 2012	TN	0	35.21	−86.74	35.21	−86.73
54	OAX	1928 UTC 14 Apr 2012	IA	0	42.14	−96.01	42.15	−96.01
54	DMX	2352 UTC 14 Apr 2012	IA	1	41.03	−94.48	41.03	−94.47
54	DMX	2353 UTC 14 Apr 2012	IA	2	41.03	−94.47	41.14	−94.2
54	DMX	0054 UTC 15 Apr 2012	IA	1	41.19	−93.67	41.19	−93.65
54	DMX	0222 UTC 15 Apr 2012	IA	1	41.25	−92.51	41.25	−92.48
54	DVN	0235 UTC 15 Apr 2012	IA	1	41.17	−92.34	41.18	−92.26
54	LBF	1805 UTC 15 Apr 2012	NE	0	41.83	−98.6	41.83	−98.61
54	LBF	1855 UTC 15 Apr 2012	NE	0	42	−98.48	42	−98.48
57	PAH	0736 UTC 30 Jan 2013	KY	2	36.68	−87.56	36.7	−87.53
59	ICT	2259 UTC 19 May 2013	KS	0	37.09	−97.06	37.1	−97.05
60	DDC	2150 UTC 20 May 2013	KS	0	37.47	−101.94	37.46	−101.94
60	EAX	2157 UTC 20 May 2013	MO	1	38.71	−93.39	38.86	−93.3
60	DDC	2205 UTC 20 May 2013	KS	0	37.51	−101.88	37.5	−101.88
60	SGF	2237 UTC 20 May 2013	MO	0	37.65	−93.83	37.66	−93.77
60	PUB	2253 UTC 20 May 2013	CO	0	37.68	−106.01	37.68	−106.01
60	SGF	0146 UTC 21 May 2013	MO	0	38.33	−92.87	38.34	−92.86
60	IND	0629 UTC 21 May 2013	IN	0	39.85	−86.73	39.85	−86.71
60	IND	0634 UTC 21 May 2013	IN	0	39.87	−86.67	39.87	−86.66
65	ILX	1825 UTC 17 Nov 2013	IL	1	38.85	−88.09	38.87	−88.02
65	IWX	2054 UTC 17 Nov 2013	IN	1	41.3	−85.8	41.32	−85.78
67	HUN	0245 UTC 21 Feb 2014	AL	1	34.69	−87.26	34.77	−87.23
72	JKL	2053 UTC 7 Oct 2014	KY	1	38.07	−83.66	38.07	−83.66
72	RNK	0339 UTC 8 Oct 2014	WV	1	37.45	−81.22	37.43	−81.12

three anonymous reviewers for their helpful comments. We also thank Dr. Alison Bridger for her guidance and support of this project and Dr. Michael Coniglio for providing an initial review of this manuscript.

Data availability statement. The tornado outbreak dataset (Anderson-Frey et al. 2018) is available from the authors upon request. Archived Level-II NEXRAD 88-D radar data are publicly available online (https://www.ncdc.noaa.gov/nexradinv/).

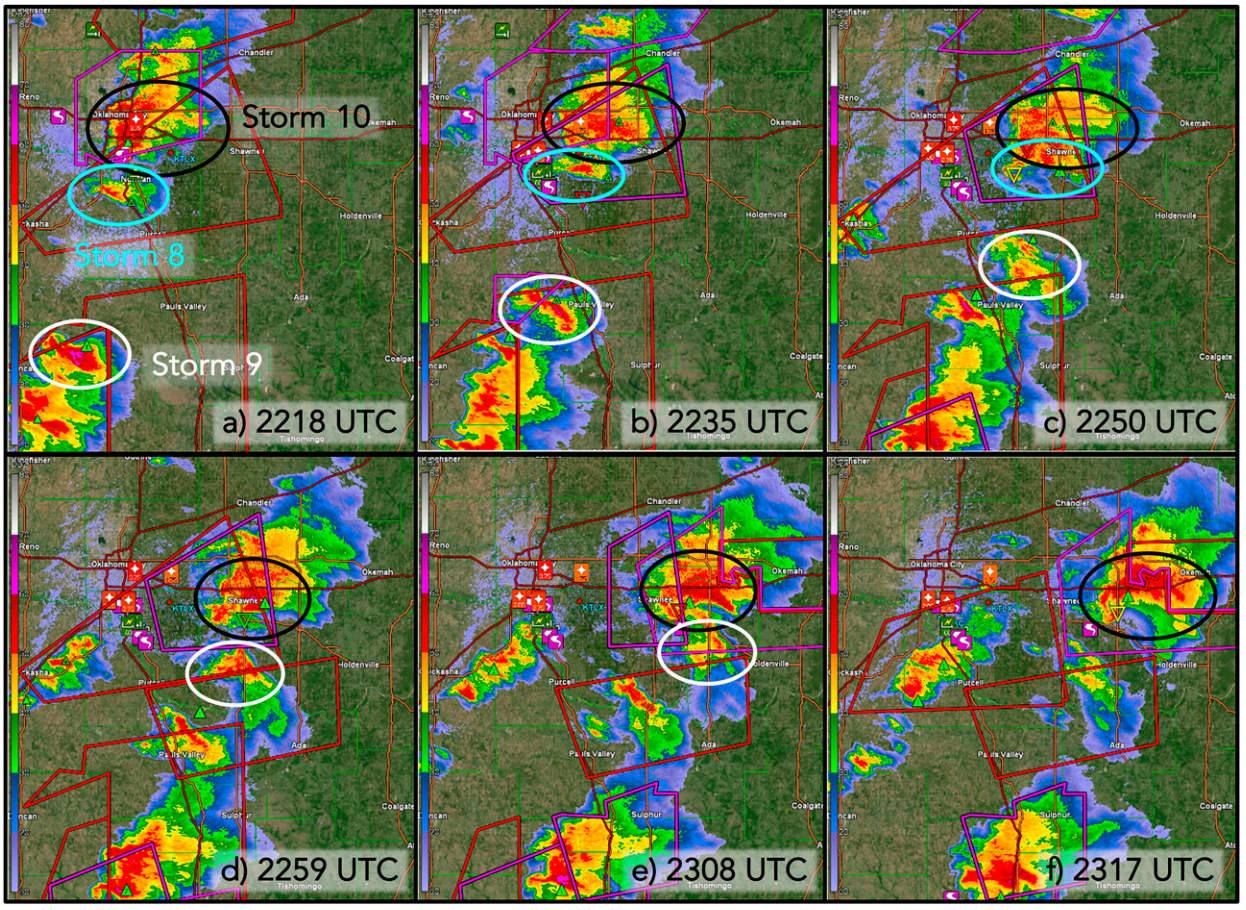

FIG. B1. An example of discrete storm identification—including storm mergers—and pairing with tornado reports during the 10 May 2010 tornado outbreak. (a)–(f) Base reflectivity from KTLX (Oklahoma City, OK) is shown, along with NWS severe thunderstorm warning (red) and tornado warning (pink) polygons. Purple squares indicate tornado reports, red and orange squares indicate hail reports, and green squares indicate wind reports. Green triangles indicate automated maximum estimated hail sizes, and upside-down triangles indicate automated tornado vortex signatures. Storms of interest are outlined in black, blue, and white, and are labeled in (a).

The NCEI tornado verification dataset is available online with NOAA credentials.

APPENDIX A

Excluded Tornado Outbreaks and Reports

The Anderson-Frey et al. (2018) dataset includes 78 tornado outbreaks from 2008 to 2014. Three of these outbreaks were not analyzed in this study due to missing radar data in the NCEI archive (10 January 2008, 19 August 2009, and 30 June 2014) that precluded identification of tornado-producing storms. This yielded a total of 75 outbreaks analyzed in this study.

Matching archived NEXRAD radar data with the NWS tornado verification database was straightforward in the overwhelming majority of cases; however, 112 tornado reports (2.7%) from the 75 outbreaks were omitted from our analysis due to spatiotemporal errors resulting in our inability to determine which storm produced the tornado. In these cases, the time and location of the tornado reports did not coincide with any storms in the radar reflectivity presentation. These reports are provided in Table A1. We do not anticipate meaningful changes in our results due to this small number of erroneous tornado reports.

APPENDIX B

Examples of Storm Object Classification

This section shows examples of how we identified distinct storm objects and paired them with tornado reports. This includes examples of discrete supercells as well as a QLCS with multiple tornadic mesovortices.

a. Discrete supercell identification and tracking (10 May 2010)

A regional supercell-tornado outbreak occurred on 10–11 May 2010 and provides an example of how we identified and tracked several tornadic supercells simultaneously, including supercell mergers. Figure B1 shows the evolution of several tornadic storms in central Oklahoma from 2218 to 2317 UTC.

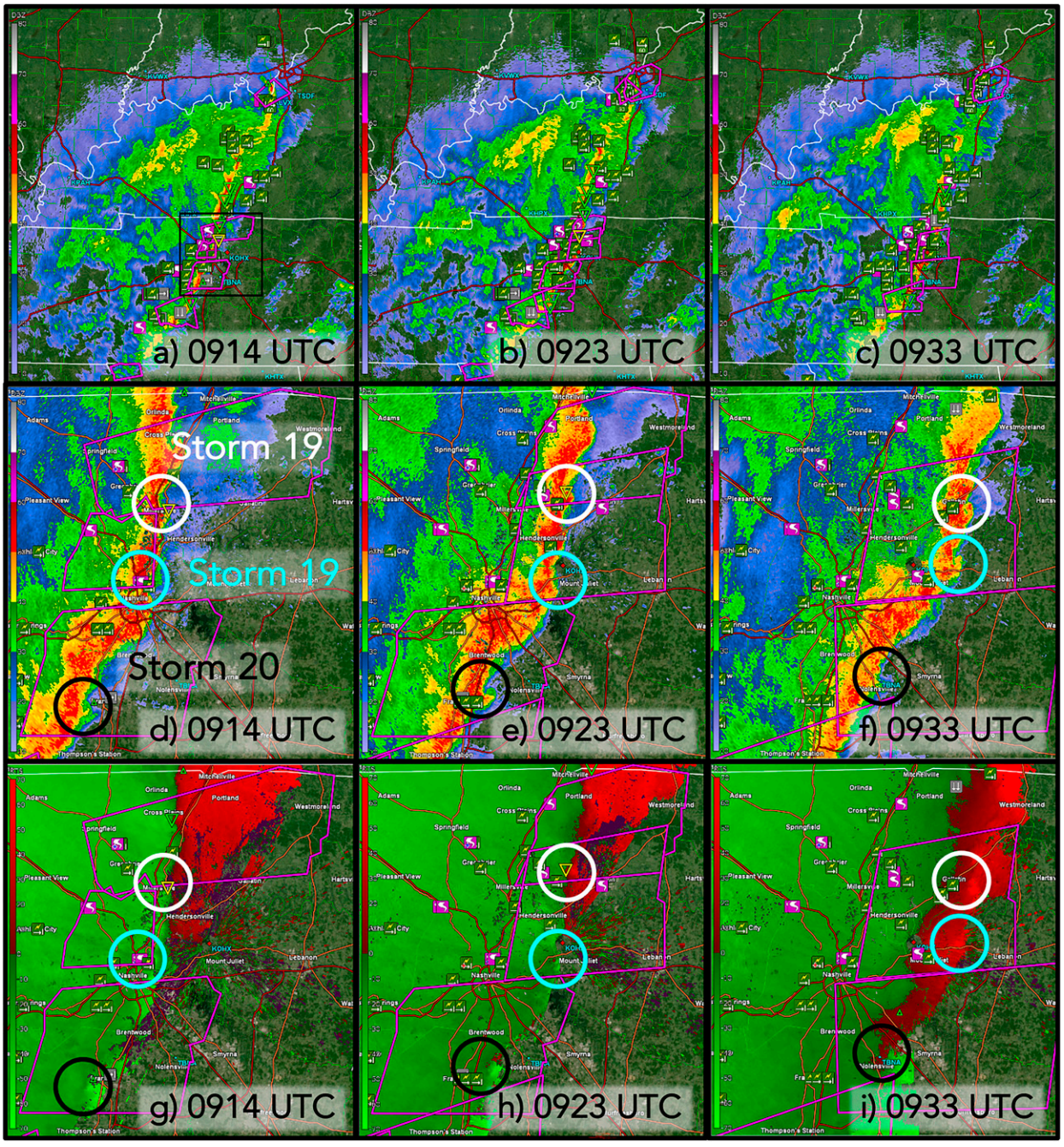

FIG. B2. As in Fig. B1, but for a mixed-mode event on 29–30 Jan 2013. (a)–(f) Base reflectivity and (g)–(i) velocity from KOHX (Old Hickory, TN) is shown at three times. A zoomed-out view is shown in (a)–(c); the black box in (a) indicates the zoomed-in region shown in (d)–(i). Three tornadic mesovortices, each associated with their own storm ID, are outlined in white, blue, and black in the zoomed-in panels and are labeled in (d).

In this case, two storms that had a history of producing tornadoes (Storm 10 circled in black, and Storm 8 circled in blue in Fig. B1a) merged around 2250–2259 UTC (Figs. B1c,d). Storm 10 previously produced tornadoes at 2220, 2222, 2227, and 2235 UTC; Storm 8 previously produced tornadoes at 2250 and 2251 UTC. The resulting storm at 2259 UTC and onward was classified as Storm 10 because the "previous" storm associated with this number produced a tornado prior to the other storm in the merger.

Later, a third tornadic supercell (Storm 9, white) moved northeastward toward Storm 10. It had a history of producing tornadoes at 2020, 2222, 2236, and 2237 UTC and merged

with Storm 10 between 2308 and 2317 UTC (Figs. B1e,f). The resulting storm was classified as Storm 9; it produced an EF3 tornado at 2311 UTC (very close to the time of the merger) and 18 tornadoes afterward.

b. QLCS mesovortex identification and tracking (29 January 2013)

A widespread tornado outbreak occurred on 29–30 January 2013 across the NWS Central and Southern Regions. Many of these tornadoes were associated with a QLCS (Figs. B2a–c), particularly in Tennessee (Figs. B2d–i). Due to the continuous linear nature of the reflectivity presentation, radial velocity observations were used to diagnose individual tornadic mesovortices—each with their own storm ID—within the QLCS.

As an example, Figs. B2d–f shows three of these mesovortices. Of the three mesovortices, the southernmost (Storm 20, circled in black) produced a tornado first at 0901 UTC and produced another tornado near Franklin, Tennessee, at 0918 UTC (Figs. B2d,e,g,h). The circulation present in the radial velocity field, as well as the small "hook" in the reflectivity presentation, helped us track this mesovortex. A second mesovortex (Storm 19, circled in blue) produced a tornado at 0912 UTC near Nashville, Tennessee (Fig. B2d). Storm 19 was tracked by following the small reflectivity notch (Figs. B2d–f) and enhanced circulation in radial velocity (Figs. B2g–i), and it produced another tornado at 0925 UTC very close to the Old Hickory, Tennessee (KOHX), radar site. Both of these tornadoes, and four more that occurred after 0933 UTC, were associated with Storm 19. Last, a third mesovortex (also labeled Storm 19, circled in white) produced tornadoes at 0910 and 0912 UTC and was located near Millersville, Tennessee, at 0914 UTC (Figs. B2d,g). We tracked Storm 19 using both reflectivity and radial velocity as it produced another tornado at 0923 UTC and an additional three tornadoes after 0933 UTC. This particular event is an example of the complexities of pairing tornado reports with QLCS circulations; in this case, both circulations identified as Storm 19 originated very close to each other (within a few kilometers) around 0845–0900 UTC (not shown). Afterward, they were sometimes included in the same tornado warning (Figs. B2f,i). For both of these reasons, these two mesovortices were identified using the same storm number.

REFERENCES

Anderson-Frey, A. K., Y. P. Richardson, A. R. Dean, R. L. Thompson, and B. T. Smith, 2016: Investigation of near-storm environments for tornado events and warnings. *Wea. Forecasting*, **31**, 1771–1790, https://doi.org/10.1175/WAF-D-16-0046.1.

——, ——, ——, ——, and ——, 2018: Near-storm environments of outbreak and isolated tornadoes. *Wea. Forecasting*, **33**, 1397–1412, https://doi.org/10.1175/WAF-D-18-0057.1.

Andra, D. L., E. M. Quoetone, and W. F. Bunting, 2002: Warning decision making: The relative roles of conceptual models, technology, strategy, and forecaster expertise on 3 May 1999. *Wea. Forecasting*, **17**, 559–566, https://doi.org/10.1175/1520-0434(2002)017<0559:WDMTRR>2.0.CO;2.

Ashley, W. S., A. J. Krmenec, and R. Schwantes, 2008: Vulnerability due to nocturnal tornadoes. *Wea. Forecasting*, **23**, 795–807, https://doi.org/10.1175/2008WAF2222132.1.

Bentley, E. S., R. L. Thompson, B. R. Bowers, J. G. Gibbs, and S. E. Nelson, 2021: An analysis of 2016–18 tornadoes and National Weather Service tornado warnings across the contiguous United States. *Wea. Forecasting*, **36**, 1909–1924, https://doi.org/10.1175/WAF-D-20-0241.1.

Brooks, H. E., and J. Correia, 2018: Long-term performance metrics for National Weather Service tornado warnings. *Wea. Forecasting*, **33**, 1501–1511, https://doi.org/10.1175/WAF-D-18-0120.1.

Brotzge, J., and S. Erickson, 2009: NWS tornado warnings with zero or negative lead times. *Wea. Forecasting*, **24**, 140–154, https://doi.org/10.1175/2008WAF2007076.1.

——, and ——, 2010: Tornadoes without NWS warning. *Wea. Forecasting*, **25**, 159–172, https://doi.org/10.1175/2009WAF2222270.1.

——, and W. Donner, 2013: The tornado warning process: A review of current research, challenges, and opportunities. *Bull. Amer. Meteor. Soc.*, **94**, 1715–1733, https://doi.org/10.1175/BAMS-D-12-00147.1.

——, S. E. Nelson, R. L. Thompson, and B. T. Smith, 2013: Tornado probability of detection and lead time as a function of convective mode and environmental parameters. *Wea. Forecasting*, **28**, 1261–1276, https://doi.org/10.1175/WAF-D-12-00119.1.

Bunkers, M. J., M. B. Wilson, M. S. Van Den Broeke, and D. J. Healey, 2022: Scan-by-scan storm-motion deviations for concurrent tornadic and nontornadic supercells. *Wea. Forecasting*, **37**, 749–770, https://doi.org/10.1175/WAF-D-21-0153.1.

Calhoun, K. M., K. L. Berry, D. M. Kingfield, T. Meyer, M. J. Krocak, T. M. Smith, G. Stumpf, and A. Gerard, 2021: The experimental warning program of NOAA's Hazardous Weather Testbed. *Bull. Amer. Meteor. Soc.*, **102**, E2229–E2246, https://doi.org/10.1175/BAMS-D-21-0017.1.

Cho, J. Y. N., J. M. Kurdzo, B. J. Bennett, M. E. Weber, J. W. Dellicarpini, A. Loconto, and H. Frank, 2022: Impact of WSR-88D intra-volume low-level scans on severe weather warning performance. *Wea. Forecasting*, **37**, 1169–1189, https://doi.org/10.1175/WAF-D-21-0152.1.

Coffer, B. E., and M. D. Parker, 2015: Impacts of increasing low-level shear on supercells during the early evening transition. *Mon. Wea. Rev.*, **143**, 1945–1969, https://doi.org/10.1175/MWR-D-14-00328.1.

——, ——, J. M. L. Dahl, L. J. Wicker, and A. J. Clark, 2017: Volatility of tornadogenesis: An ensemble of simulated nontornadic and tornadic supercells in VORTEX2 environments. *Mon. Wea. Rev.*, **145**, 4605–4625, https://doi.org/10.1175/MWR-D-17-0152.1.

Edwards, R., 2012: Tropical cyclone tornadoes: A review of knowledge in research and prediction. *Electron. J. Severe Storms Meteor.*, **7** (6), https://ejssm.com/ojs/index.php/site/article/view/42 .

Flournoy, M. D., M. C. Coniglio, E. N. Rasmussen, J. C. Furtado, and B. E. Coffer, 2020: Modes of storm-scale variability and tornado potential in VORTEX2 near- and far-field tornadic environments. *Mon. Wea. Rev.*, **148**, 4185–4207, https://doi.org/10.1175/MWR-D-20-0147.1.

Gallo, B. T., and Coauthors, 2022: Exploring the watch-to-warning space: Experimental outlook performance during the 2019 spring forecasting experiment in NOAA's Hazardous Weather

Testbed. *Wea. Forecasting*, **37**, 617–637, https://doi.org/10.1175/WAF-D-21-0171.1.

Kingfield, D. M., and M. M. French, 2022: The influence of WSR-88D intra-volume scanning strategies on thunderstorm observations and warnings in the dual-polarization radar era: 2011–20. *Wea. Forecasting*, **37**, 283–301, https://doi.org/10.1175/WAF-D-21-0127.1.

Klees, A. M., Y. P. Richardson, P. M. Markowski, C. Weiss, J. M. Wurman, and K. K. Kosiba, 2016: Comparison of the tornadic and nontornadic supercells intercepted by VORTEX2 on 10 June 2010. *Mon. Wea. Rev.*, **144**, 3201–3231, https://doi.org/10.1175/MWR-D-15-0345.1.

Krocak, M. J., and H. E. Brooks, 2018: Climatological estimates of hourly tornado probability for the United States. *Wea. Forecasting*, **33**, 59–69, https://doi.org/10.1175/WAF-D-17-0123.1.

——, and ——, 2021: The influence of weather watch type on the quality of tornado warnings and its implications for future forecasting systems. *Wea. Forecasting*, **36**, 1675–1680, https://doi.org/10.1175/WAF-D-21-0052.1.

——, J. N. Allan, J. T. Ripberger, C. L. Silva, and H. C. Jenkins-Smith, 2021a: An analysis of tornado warning reception and response across time: Leveraging respondent's confidence and a nocturnal tornado climatology. *Wea. Forecasting*, **36**, 1649–1660, https://doi.org/10.1175/WAF-D-20-0207.1.

——, M. D. Flournoy, and H. E. Brooks, 2021b: Examining subdaily tornado warning performance and associated environmental characteristics. *Wea. Forecasting*, **36**, 1779–1784, https://doi.org/10.1175/WAF-D-21-0097.1.

Lebel, L. J., and P. M. Markowski, 2023: An analysis of the impact of vertical wind shear on convection initiation using large-eddy simulations: Importance of wake entrainment. *Mon. Wea. Rev.*, https://doi.org/10.1175/MWR-D-22-0176.1, in press.

Markowski, P. M., 2020: What is the intrinsic predictability of tornadic supercell thunderstorms? *Mon. Wea. Rev.*, **148**, 3157–3180, https://doi.org/10.1175/MWR-D-20-0076.1.

Peters, J. M., H. Morrison, T. C. Nelson, J. N. Marquis, J. P. Mulholland, and C. J. Nowotarski, 2022a: The influence of shear on deep convection initiation. Part I: Theory. *J. Atmos. Sci.*, **79**, 1669–1690, https://doi.org/10.1175/JAS-D-21-0145.1.

——, ——, ——, ——, ——, and ——, 2022b: The influence of shear on deep convection initiation. Part II: Simulations. *J. Atmos. Sci.*, **79**, 1691–1711, https://doi.org/10.1175/JAS-D-21-0144.1.

Quoetone, E., J. Boettcher, and C. Spannagle, 2009: How did that happen? A look at factors that go into forecaster warning decisions. Extended Abstracts, *34th Annual Meeting*, Norfolk, VA, National Weather Association, https://nwas.org/annual-meeting-events/past-meetings/2009-annual-meeting/.

Rotunno, R., and J. Klemp, 1985: On the rotation and propagation of simulated supercell thunderstorms. *J. Atmos. Sci.*, **42**, 271–292, https://doi.org/10.1175/1520-0469(1985)042<0271:OTRAPO>2.0.CO;2.

Schenkel, B. A., R. Edwards, and M. Coniglio, 2020: A climatological analysis of ambient deep-tropospheric vertical wind shear impacts upon tornadoes in tropical cyclones. *Wea. Forecasting*, **35**, 2033–2059, https://doi.org/10.1175/WAF-D-19-0220.1.

——, M. Coniglio, and R. Edwards, 2021: How does the relationship between ambient deep-tropospheric vertical wind shear and tropical cyclone tornadoes change between coastal and inland environments? *Wea. Forecasting*, **36**, 539–566, https://doi.org/10.1175/WAF-D-20-0127.1.

Shafer, C. M., and C. A. Doswell III, 2011: Using kernel density estimation to identify, rank, and classify severe weather outbreak events. *Electron. J. Severe Storms Meteor.*, **6** (2), https://doi.org/10.55599/ejssm.v6i2.29.

Skinner, P. S., and Coauthors, 2018: Object-based verification of a prototype Warn-on-Forecast System. *Wea. Forecasting*, **33**, 1225–1250, https://doi.org/10.1175/WAF-D-18-0020.1.

Smith, B. T., R. L. Thompson, J. S. Grams, C. Broyles, and H. E. Brooks, 2012: Convective modes for significant severe thunderstorms in the contiguous United States. Part I: Storm classification and climatology. *Wea. Forecasting*, **27**, 1114–1135, https://doi.org/10.1175/WAF-D-11-00115.1.

——, ——, A. R. Dean, and P. T. Marsh, 2015: Diagnosing the conditional probability of tornado damage rating using environmental and radar attributes. *Wea. Forecasting*, **30**, 914–932, https://doi.org/10.1175/WAF-D-14-00122.1.

Trujillo-Falcón, J. E., J. Reedy, K. E. Klockow-McClain, K. L. Berry, G. J. Stumpf, A. V. Bates, and J. G. LaDue, 2022: Creating a communication framework for FACETs: How probabilistic hazard information affected warning operations in NOAA's Hazardous Weather Testbed. *Wea. Climate Soc.*, **14**, 881–892, https://doi.org/10.1175/WCAS-D-21-0136.1.

Wilson, K. A., B. T. Gallo, P. Skinner, A. Clark, P. Heinselman, and J. J. Choate, 2021: Analysis of end user access of Warn-on-Forecast guidance products during an experimental forecasting task. *Wea. Climate Soc.*, **13**, 859–874, https://doi.org/10.1175/WCAS-D-20-0175.1.